



Circuits and Systems for Receiving, Transmitting and Signal Processing

DOI: 10.18721/JCSTCS.13403

УДК 621.373.52

PHASE NOISE OF A MICROSTRIP MICROWAVE OSCILLATOR WITH VARACTOR FREQUENCY TUNING 6–12 GHz

A.B. Nikitin, E.I. Khabitueva

Peter the Great St. Petersburg Polytechnic University,
St. Petersburg, Russian Federation

This work presents the results of a study of the microwave oscillator's active device biasing influence on the oscillator phase noise. The paper considers a hybrid voltage-controlled oscillator (VCO) with an octave frequency tuning (6–12 GHz), based on a low-noise SiGe-heterojunction transistor. The simulation of the VCO in the AWR Design Environment (AWR DE) allowed one to evaluate the choice of the transistor operating point influence on the oscillator phase noise. Based on the data obtained, an experimental study of the fluctuation characteristics of several samples of the hybrid microwave VCOs, differing in the operating mode of the active devices, was carried out. The results of the research carried out make it possible to determine a number of conditions (the value of the collector current, the ratio between the currents of the transistor base and the resistive divider, determining the mode of the active device), which provide the best oscillator characteristics. It is shown that the smallest average level of the phase noise power spectral density is -95 dBc/Hz at 100 kHz offset from the carrier with a minimum change in its level in the tuning range within ± 2.5 dB.

Keywords: microwaves, voltage-controlled oscillator, VCO, phase noise, fluctuation characteristics.

Citation: Nikitin A.B., Khabitueva E.I. Phase noise of a microstrip microwave oscillator with varactor frequency tuning 6–12 GHz. Computing, Telecommunications and Control, 2020, Vol. 13, No. 4, Pp. 34–43. DOI: 10.18721/JCSTCS.13403

This is an open access article under the CC BY-NC 4.0 license (<https://creativecommons.org/licenses/by-nc/4.0/>).

ФАЗОВЫЙ ШУМ МИКРОПОЛОСКОВОГО СВЧ-ГЕНЕРАТОРА С ВАРАКТОРНОЙ ПЕРЕСТРОЙКОЙ ЧАСТОТЫ 6–12 ГГц

А.Б. Никитин, Е.И. Хабитуева

Санкт-Петербургский политехнический университет Петра Великого,
Санкт-Петербург, Российская Федерация

Описаны результаты исследования влияния режима работы активного элемента СВЧ-генератора, управляемого напряжением (ГУН), на его флуктуационные характеристики. Рассмотрен автогенератор с октавной перестройкой частоты выходного колебания (6–12 ГГц), выполненный на основе гибридной технологии на базе малошумящего SiGe-гетеропереходного транзистора. Проведённое моделирование ГУН в среде AWR Design Environment (AWR DE) позволило оценить влияние выбора рабочей точки транзистора на уровень фазового шума автогенератора. На основе полученных данных проведено экспериментальное исследование флуктуационных характеристик нескольких образцов перестраиваемых генераторов, отличающихся режимом работы активного элемента. Определён ряд условий (величина коллекторного тока, соотношение между токами базы транзистора и резистивного делителя, определяющего режим активного элемента), обеспечивающих наилучшие флуктуационные характеристики. Показано,

что наименьший средний уровень спектральной плотности мощности фазовых шумов (СПМ ФШ) составляет -95 дБн/Гц на частоте отстройки от несущей 100 кГц при минимальном (в пределах $\pm 2,5$ дБ) изменении СПМ ФШ в диапазоне перестройки.

Ключевые слова: СВЧ, генератор, управляемый напряжением, ГУН, флуктуационные характеристики, фазовый шум.

Ссылка при цитировании: Никитин А.Б., Хабитуева Е.И. Фазовый шум микрополоскового СВЧ-генератора с варакторной перестройкой частоты $6\text{--}12$ ГГц // Computing, Telecommunications and Control. 2020. Vol. 13. No. 4. Pp. 34–43. DOI: 10.18721/JCSTCS.13403

Статья открытого доступа, распространяемая по лицензии CC BY-NC 4.0 (<https://creativecommons.org/licenses/by-nc/4.0/>).

Introduction

Design of a stable wideband microwave source based on frequency synthesizers with phase-locked loop (PLL) implies the use of low-noise voltage-controlled oscillators (VCOs) with ultra-wide band (octave or more) frequency tuning range in such systems [1–7]. At the same time, fluctuation characteristics of VCOs are to a significant degree determined by the choice of oscillator's active device. For example, in hybrid microwave oscillators it is advisable to use SiGe-heterojunction bipolar transistors characterized by the lowest levels of phase noise with oscillation frequencies up to $10\text{--}15$ GHz [7].

In addition, oscillator's operation heavily depends on the mode of the active device related to the choice of the transistor's operating point and bias circuit. Thus, for example, in the simplest circuit with fixed current bias, the operating point position, and therefore, the oscillator's characteristics are significantly affected by the specific transistor and environment temperature [8].

One of the ways to eliminate this negative effect is to use bias circuit with emitter resistor, that provides (be means of serial DC-coupled negative feedback in the circuit) stability of the operating point position, and therefore, the oscillator's parameters in a wide range of temperatures. This also allows to replace an active device without the consequent replacement of the whole circuit [8].

It should be noted that in scientific publications, this kind of circuit is most frequently considered in terms of its application not in oscillators, but in various amplifiers [9–14]. Indeed, paper [14] presents general recommendations as to the choice of the bias circuit parameters and describes their influence on operation of amplifiers built on the basis of bipolar transistors.

In the papers devoted to the topic under consideration, the authors, in general, describe monolithic microwave integrated circuit (MMIC) oscillators. In addition, the study of hybrid microwave VCOs permitting the use of simpler manufacturing process is usually restricted to considering devices intended for operation in the frequency range significantly less than an octave [1, 15–20]. At the same time, the tuning of VCOs in wide and ultra-wide band (octave or more) frequency range results in a considerable change in the conditions of active device operation which hinders the choice of the mode providing the best fluctuation characteristics.

Moreover, publications often present results of analyzing the influence of active device circuit and mode on oscillator's characteristics (frequency response, fluctuation, etc.) without any experimental verification which puts limitations on practical application of such data [1, 21, 22].

This article contains study results on the dependence of phase noise power spectral density $S(F)$ of octave microwave oscillator in the $6\text{--}12$ GHz range on active device operating mode [23, 24]. The tunable oscillator is hybrid based on low-noise SiGe-heterojunction bipolar transistor NESG3031M14 [25].

Computation of VCO parameters

Fig. 1a shows a layout of the microwave oscillator under consideration. Fig. 1b presents a fragment of its simplified circuit which contains a transistor and resistive elements determining active device operating mode (R_1 , R_2 и R_E). Fig. 1c shows characteristics of the VCO.

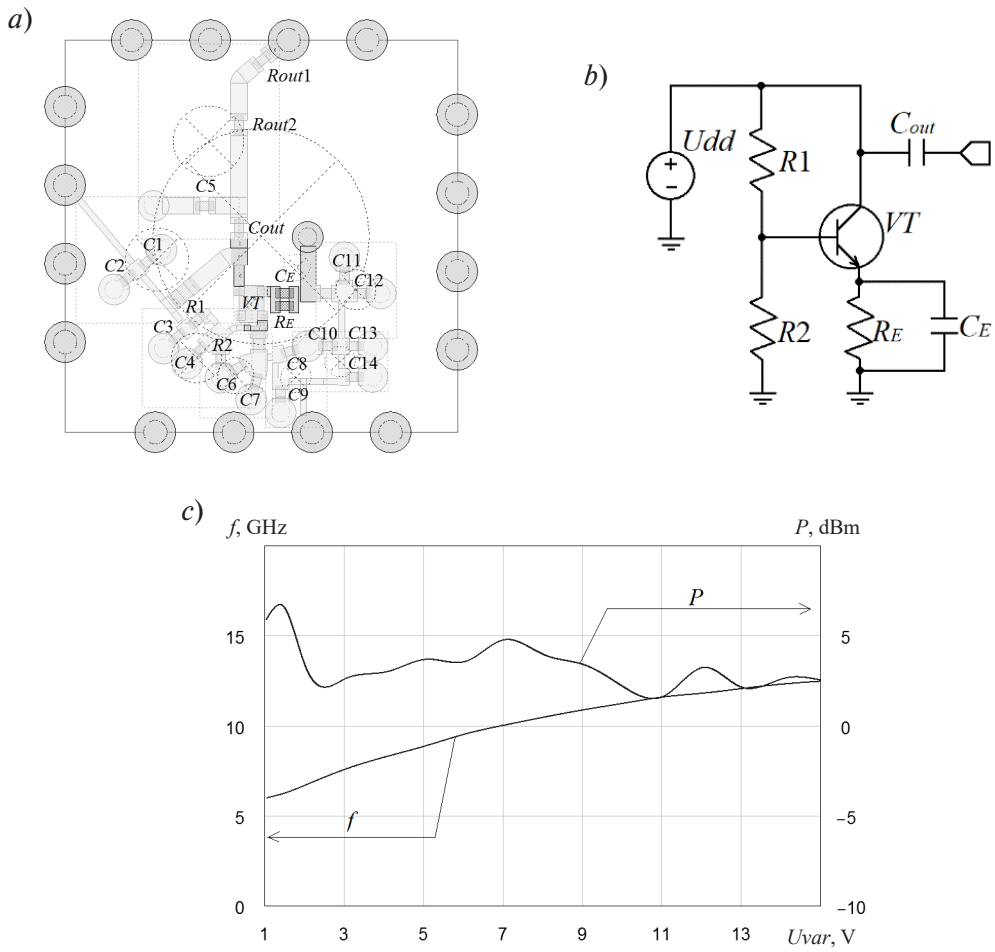


Fig. 1. VCO: *a* – layout; *b* – simplified circuit without frequency control elements;
c – dependence of oscillation frequency f and power P on control voltage U_{var}

To compute resistance values of resistors R_1 , R_2 and R_E , determining transistor mode VT (Fig. 1), we use the following expressions [1, 14]:

$$R_1 = \frac{U_{R1}}{I_1} = \frac{U_{dd} - U_{R2}}{I_1} = \frac{U_{dd} - U_{R2}}{kI_B^0}, \quad (1)$$

$$R_2 = \frac{U_{R2}}{I_2} = \frac{U_{R_E} + U_{BE}^0}{I_2} = \frac{U_{R_E} + U_{BE}^0}{(k-1)I_B^0}, \quad (2)$$

$$R_E = \frac{U_{R_E}}{I_E} = \frac{U_{dd} - U_{CE}^0}{I_C^0 + I_B^0}, \quad (3)$$

where U_{dd} is supply voltage of the VCO; U_{R1} , U_{R2} and U_{R_E} are voltage across resistors R_1 , R_2 and R_E , respectively; I_1 , I_2 and I_E are current across resistors R_1 , R_2 and R_E ; I_B^0 and I_C^0 are base and collector current of the transistor; U_{BE}^0 and U_{CE}^0 are base-emitter and collector-emitter voltages of the transistor; k is coefficient of proportionality between I_1 and I_B^0 values.

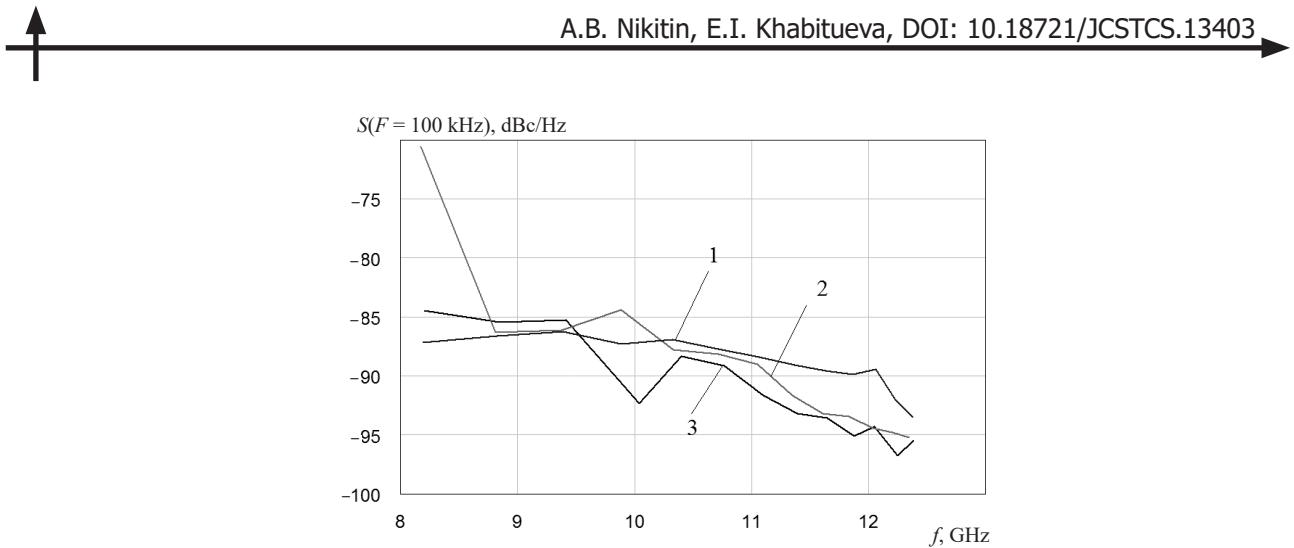


Fig. 2. VCO's simulation characteristics

To minimize possible unwanted spectral components in the output oscillations, the value of U_{CE}^0 needs to be approximately half of the VCO supply voltage. Moreover, for the NESG3031M14 transistor, I_B^0 and I_C^0 values should be more than 20 μ A and 6 mA, respectively [8].

To enhance bias voltage stability supplied to the transistor base (using voltage divider R_1-R_2 , see Fig. 1), it is advisable that the value of the current across resistors R_1 and R_2 was sufficiently high, which requires increasing k parameter value (expressions (1), (2)). However, one should make allowance for the fact that excessively high divider current may result in inadequate power consumption and, consequently, a drop in efficiency.

Keeping in mind these remarks, as well as parameters of NESG3031M14 transistor used in the 6–12 GHz VCO [25], we obtained several options of oscillator's circuit configuration corresponding to different positions of the operating point. As an example, in Fig. 2, we demonstrate a diagram of dependence of $S(F = 100 \text{ kHz})$ on VCO's frequency values obtained as a result of modeling in AWR DE [26], for several options of transistor point position.

The dependencies presented in Fig. 2 correspond to the following cases:

- curve 1: $I_C^0 = 11 \text{ mA}$, $U_{CE}^0 = 2 \text{ V}$, $I_B^0 = 40 \mu\text{A}$, $U_{BE}^0 = 0.845 \text{ V}$, $k = 5$ ($R_1 = 5.8 \text{ kOhm}$, $R_2 = 22 \text{ kOhm}$, $R_E = 240 \text{ Ohm}$);
- curve 2: $I_C^0 = 20 \text{ mA}$, $U_{CE}^0 = 2 \text{ V}$, $I_B^0 = 80 \mu\text{A}$, $U_{BE}^0 = 0.87 \text{ V}$, $k = 5$ ($R_1 = 2.9 \text{ kOhm}$, $R_2 = 11 \text{ kOhm}$, $R_E = 130 \text{ Ohm}$);
- curve 3: $I_C^0 = 30 \text{ mA}$, $U_{CE}^0 = 2.5 \text{ V}$, $I_B^0 = 140 \mu\text{A}$, $U_{BE}^0 = 0.875 \text{ V}$, $k = 5$ ($R_1 = 2.3 \text{ kOhm}$, $R_2 = 5.5 \text{ kOhm}$, $R_E = 75 \text{ Ohm}$).

Fig. 2 shows that reduction of $S(F)$ (for the same value of k parameter) is possible if collector current I_C^0 is increased. Thus, for example, a change in I_C^0 value from 11 mA up to 20 mA allows to reduce the level of $S(F)$ by (2–4) dB in the most part of the tuning range.

At the same time, it should be noted that voltage values between the collector and transistor emitter $U_{CE}^0 = 2.5 \text{ V}$ and $U_{CE}^0 = 2 \text{ V}$ do not provide the required octave (6–12 GHz) tuning range of the oscillator's output frequency.

Further research of the VCO revealed that reduction of $S(F)$ (by several dB) is possible in case of an increase not only in the collector current, but in parameter k as well.

Thus, the modeling of several VCO circuits corresponding to different positions of the operating point performed in AWR DE showed that the phase noise reduction is connected with the increase of collector current and coefficient k . In addition, to provide the needed tuning range of the oscillator, it is necessary that $U_{CE}^0 > 2.5 \text{ V}$.

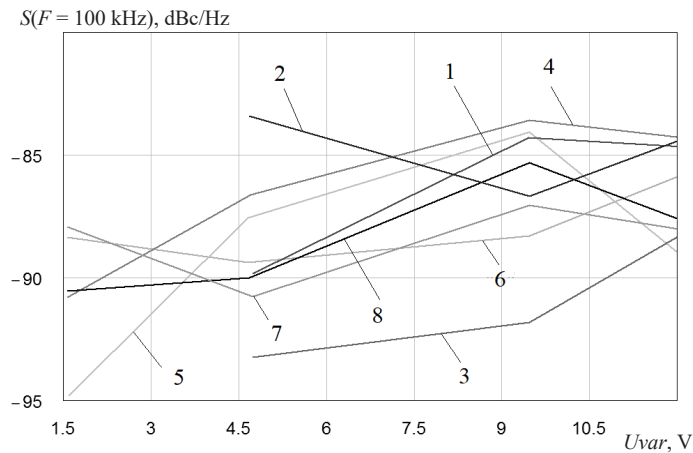


Fig. 3. VCO's measured characteristics

Experimental study of VCO's phase noise

For the experimental study of the VCO samples, we used N9000A CXA series signal analyzer by Keysight Technologies [27], designed for operation in the range from 9 kHz to 26.5 GHz.

In Fig. 3 we present measured VCO's fluctuation characteristics for several options of transistor point position.

The dependencies presented in Fig. 3 correspond to the following cases:

- curve 1: $I_C^0 = 11 \text{ mA}$, $U_{CE}^0 = 2 \text{ V}$, $I_B^0 = 40 \mu\text{A}$, $U_{BE}^0 = 0.845 \text{ V}$, $k = 5$ ($R_1 = 5.8 \text{ kOhm}$, $R_2 = 22 \text{ kOhm}$, $R_E = 240 \text{ Ohm}$);
- curve 2: $I_C^0 = 20 \text{ mA}$, $U_{CE}^0 = 2 \text{ V}$, $I_B^0 = 80 \mu\text{A}$, $U_{BE}^0 = 0.87 \text{ V}$, $k = 5$ ($R_1 = 2.9 \text{ kOhm}$, $R_2 = 11 \text{ kOhm}$, $R_E = 130 \text{ Ohm}$);
- curve 3: $I_C^0 = 30 \text{ mA}$, $U_{CE}^0 = 2 \text{ V}$, $I_B^0 = 140 \mu\text{A}$, $U_{BE}^0 = 0.88 \text{ V}$, $k = 5$ ($R_1 = 1.65 \text{ kOhm}$, $R_2 = 6.4 \text{ kOhm}$, $R_E = 90 \text{ Ohm}$);
- curve 4: $I_C^0 = 20 \text{ mA}$, $U_{CE}^0 = 2.5 \text{ V}$, $I_B^0 = 80 \mu\text{A}$, $U_{BE}^0 = 0.85 \text{ V}$, $k = 5$ ($R_1 = 4.02 \text{ kOhm}$, $R_2 = 7.5 \text{ kOhm}$, $R_E = 75 \text{ Ohm}$);
- curve 5: $I_C^0 = 30 \text{ mA}$, $U_{CE}^0 = 2.5 \text{ V}$, $I_B^0 = 140 \mu\text{A}$, $U_{BE}^0 = 0.875 \text{ V}$, $k = 5$ ($R_1 = 2.3 \text{ kOhm}$, $R_2 = 5.5 \text{ kOhm}$, $R_E = 75 \text{ Ohm}$);
- curve 6: $I_C^0 = 30 \text{ mA}$, $U_{CE}^0 = 3 \text{ V}$, $I_B^0 = 140 \mu\text{A}$, $U_{BE}^0 = 0.875 \text{ V}$, $k = 5$ ($R_1 = 3 \text{ kOhm}$, $R_2 = 4.5 \text{ kOhm}$, $R_E = 56 \text{ Ohm}$);
- curves 7 and 8: $I_C^0 = 33 \text{ mA}$, $U_{CE}^0 = 3 \text{ V}$, $I_B^0 = 160 \mu\text{A}$, $U_{BE}^0 = 0.88 \text{ V}$, $k = 5$ ($R_1 = 2.7 \text{ kOhm}$, $R_2 = 4.02 \text{ kOhm}$, $R_E = 51 \text{ Ohm}$).

Fig. 3 shows that:

1. For the voltage values across the transistor collector $U_{CE}^0 < 3 \text{ V}$, it is impossible to provide the required frequency range tuning to the VCO: 6–12 GHz. Moreover, for $U_{CE}^0 = 2.5 \text{ V}$ in the lower end of the range (when $Uvar < 1.4 \text{ V}$), we can observe a spectrum collapse. Therefore, in order to provide the oscillator under consideration with frequency tuning across the whole bandwidth, the operating voltage U_{CE}^0 needs to be no less than 3 V.
2. The level of the phase noise power spectral density drops as the collector current I_C^0 increases. Taking this fact into account, as well as keeping the transistor data, limiting the maximum value of the collector current, the operating value of I_C^0 needs to be no more than 30 mA.

We carried out further experiments for the purpose of studying the influence of the ratio between the base current I_B^0 and resistive divider R_1-R_2 on VCO's phase noise for the selected values of collector-emitter voltage and collector current: $U_{CE}^0 = 3 \text{ V}$, $I_C^0 = 30 \text{ mA}$.

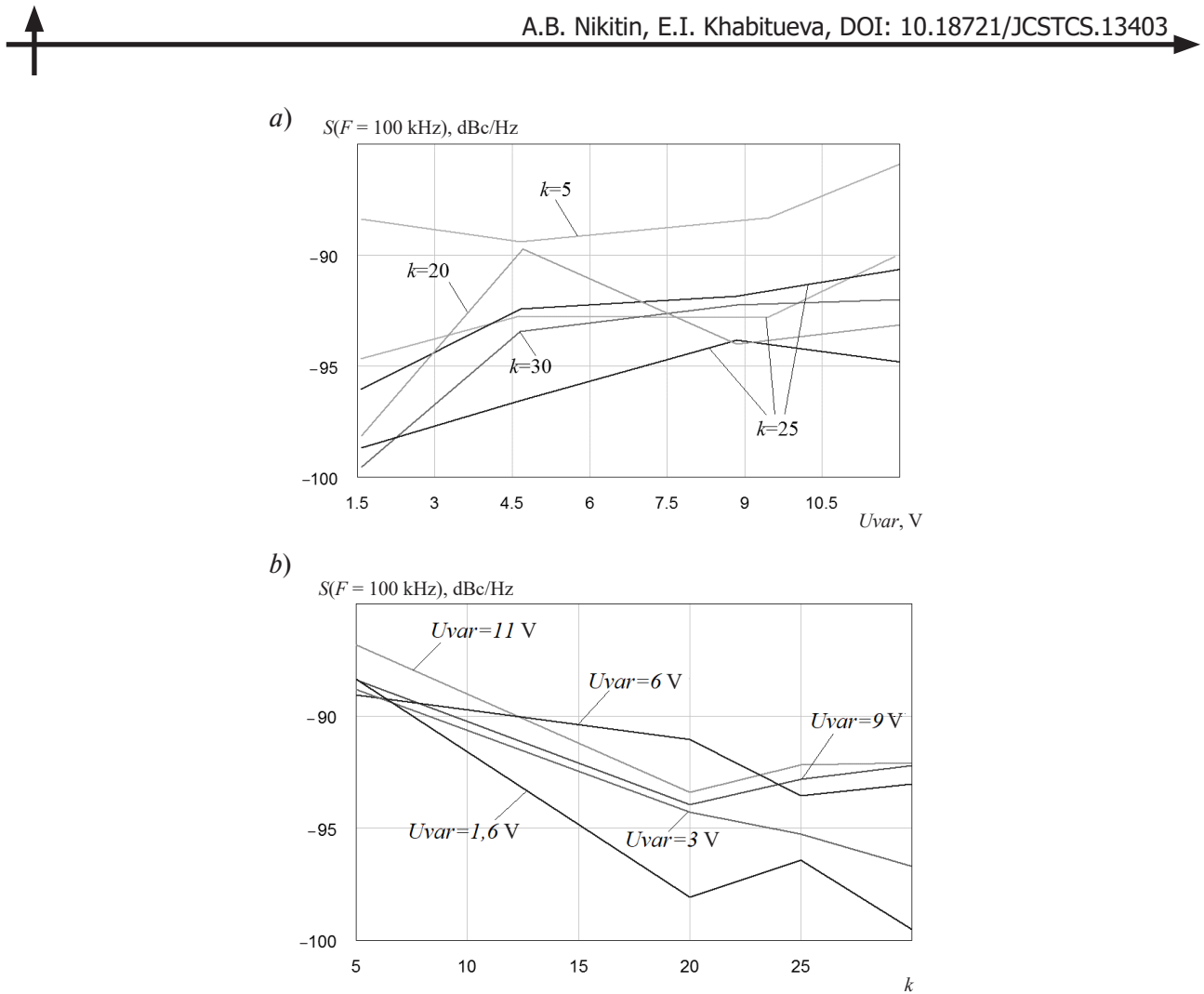


Fig. 4. VCO's measured characteristics for different k values

Fig. 4 shows VCO's measured characteristics at $U_{CE}^0 = 3 \text{ V}$ and $I_C^0 = 30 \text{ mA}$.

Fig. 4a shows that for constant values of collector voltage and current of the transistor, the ratio between the base and resistive divider currents may have significant influence on the fluctuation characteristics of the VCO. For example, in the lower end of the tuning range an increase of the parameter k from 5 to 30 allows us to reduce the noise level by more than 10 dB. At the same time, the minimum level of $S(F)$ amounts to a value of -100 dBc/Hz order at 100 kHz offset from the carrier.

Fig. 4b shows that when $k = 25$, we observe the lowest change in $S(F)$ in the tuning band: around $\pm 2.5 \text{ dB}$ with the average level around -95 dBc/Hz . Note that the obtained results are on a par with characteristics of foreign VCO samples of the similar application [28].

Thus, the data obtained as a result of experimental research of the fluctuation characteristic of a 6–12 GHz microwave oscillator are in full compliance with the results of computer modeling of the VCO in the AWR Design Environment. For instance, the identified dependencies of phase noise level on the value of collector current and parameter k , according to which a reduction of VCO's phase noises is possible if I_C^0 and k increase, were proved experimentally: the computations showed that an increase in collector current from 11 mA up to 30 mA (curves 1 and 3 in Fig. 3) provides a reduction of $S(F)$ by more than 4 dB.

Conclusion

As a result of studying a hybrid microwave VCO with an octave frequency tuning, we determined its operating conditions providing the best fluctuation characteristics. The paper showed the mode of the

oscillator's active device based on a SiGe-heterojunction transistor, which provides the minimal level of phase noise of the output oscillation in the range of 6–12 GHz, is achieved if the following conditions are satisfied:

- Maximum possible collector current: $I_C^0 = 30$ mA.
- Voltage U_{CE}^0 ensuring the entire range of frequency tuning: $U_{CE}^0 = 3$ V.
- Ratio of divider and base currents of the transistor $k = 25$. Such a value of coefficient k ensures the minimum average level of phase noise: around -95 dBc/Hz at 100 kHz offset from the carrier with a minimum (within ± 2.5 dB) change in $S(F)$ in the tuning range.

The obtained results could be used in design of hybrid microwave oscillators providing frequency tuning in a range of an octave or more.

REFERENCES

1. **Grebennikov A.V.** *RF and Microwave. Transistor oscillator design*. John Wiley & Sons, Ltd., 2007. 441 p.
2. **Khanna A.P.S.** State of the art in microwave VCOs. *Microwave Journal*, 2015, Vol. 58, No. 5, Pp. 22–42.
3. **Chenakin A.** Frequency synthesis: Current status and future projections. *Microwave Journal*, 2017, Vol. 60, No. 4, Pp. 22–36.
4. **Chenakin A.** Select a VCO or YIG for a PLL Synthesizer. *Microwaves and RF*, 2016. Vol. 55, No. 2, Pp. 2–6.
5. **Garghetti A., Quadrelli F., Bassi M., Mazzanti A.** Impact of the base resistance noise and design of a -190 -dBc/Hz FoM Bipolar Class-C VCO. *IEEE Solid-State Circuits Letters*, 2020, Vol. 3, Pp. 90–93. DOI: 10.1109/LSSC.2020.3006484
6. **Gorevoy A.V.** Vybor generatorov dlya postroyeniya maloshumyashchikh SVCh-sintezatorov [Select an oscillator for a low noise microwave synthesizer]. *Komponenty i Tekhnologii [Components & Technologies]*, 2012, No. 6, Pp. 12–17. (rus)
7. **Gorevoy A.V.** Generator diapazona 1-2 GGts s povyshennoy krutiznoy regulirovochnoy kharakteristiki [1-2 GHz range oscillator with increased control slope]. *Doklady TUSURa [TUSUR University Proceedings]*, 2011, No. 1 (23), Pp. 44–49. (rus)
8. **Milovzorov O.V., Pankov I.G.** *Elektronika [Electronics]*. Moscow: Vysshaya shkola Publ., 2008. 288 p. (rus)
9. **Datta K., Hashemi H.** Waveform engineering in a mm-wave stacked-HBT switching power amplifier. *2017 IEEE Radio Frequency Integrated Circuits Symposium (RFIC)*, 2017.
10. **Stärke P., Steinweg L., Carta C., Ellinger F.** Common emitter low noise amplifier with 19 dB Gain for 140 GHz to 220 GHz in 130 nm SiGe. *International Conference on Wireless and Mobile Computing, Networking and Communications (WiMob)*, 2019.
11. **Coen C.T., Ulusoy A.Ç., Song P., Ildefonso A., Kaynak M., Tillack B., Cressler J.D.** Design and on-wafer characterization of G-Band SiGe HBT low-noise amplifiers. *IEEE Transactions on Microwave Theory and Techniques*, 2016, Vol. 64, Iss. 11, Pp. 3631–3642.
12. **Pandiev I.M., Stoimenov E.C.** Design and development of low-power multistage amplifier laboratory kit for electronic engineering education. *X National Conference with International Participation (ELECTRONICA)*, 2019.
13. **Pietron D., Butrym I., Wiechowski L., Pleskacz W.A.** Design of a wideband low noise amplifier for a FMCW synthetic aperture radar in 130 nm SiGe BiCMOS technology. *25th International Conference on Mixed Design of Integrated Circuits and System (MIXDES)*, 2018.
14. **Asmolov G.I., Rozhkov V.M., Lobov O.P.** *Usilitelnyye skhemy v sistemakh transportnoy telematiki [Amplifying circuits in transport telematics systems]*. Moscow: MADI Publ., 2015. 88 p. (rus)
15. **Perez J.C., Guardado A.H., Freixedas J.C., Ambrojo J.C.P.** A hybrid bipolar wideband VCO with line-averaged tuning behaviour for a new generation TTC transponder. *48th European Microwave Conference (EuMC)*, 2018, Pp. 1341–1344.

16. **Singha H., Parmara Y.o, Rajb V.B., Pandya H.M., Kumara J., Mishra M., Nimala A.T., Sharmaa M.U.** Sensitivity enhancement studies of SAW vapor sensor by oscillator tuning using varactor diode. *IEEE Sensors Journal*, 2016, Vol. 17, No. 5, Pp. 1391–1398.
17. **Patel S.S., Gupta S., Ghodgaonkar D.** Ku-band novel voltage controlled oscillator microwave integrated circuit with low phase noise. *2014 International Conference on Computational Intelligence and Communication Networks*, 2014, Pp. 74–77.
18. **Dyskin A., Wagner S., Kallfass I.** A compact resistive quadrature low noise Ka-band VCO SiGe HBT MMIC. *12th German Microwave Conference (GeMiC)*, 2019.
19. **Florian C., D'Angelo S., Scappaviva F.** A chip set of low phase noise MMIC VCOs at C, X and Ku-band in InGaP-GaAs HBT technology for satellite telecommunications. *2017 IEEE MTT-S International Microwave Symposium (IMS)*.
20. **Fanori L., Andreani P.** Highly efficient class-C CMOS VCOs, including a comparison with class-B VCOs. *IEEE Journal of Solid-State Circuits*, 2013, Vol. 48, Iss. 7, Pp. 1730–1740.
21. **Habbachi N., Boukabache A., Boussetta H., Pons P., Kallala M.A., Besbes K.** Analyzes of VCO performances based on RF spiral inductors. *2017 International Conference on Engineering & MIS (ICEMIS)*, 2018.
22. **Maffezzoni P., Levantino S.** Analysis of VCO phase noise in charge-pump phase-locked loops. *IEEE Transactions on Circuits and Systems I*, 2012, Vol. 59, Iss. 10, Pp. 2165–2175.
23. **Nikitin A.B., Khabitueva E.I.** Sverkhshirokopolosnyy SVCh-generator, upravlyayemyy napryazheniyem [Ultrawideband microwave voltage-controlled oscillator]. *Radiotekhnika*, 2018, No. 1, Pp. 4–9. (rus)
24. **Nikitin A.B., Khabitueva E.I.** The features of design of an ultra-wideband microwave hybrid VCO. *Computing, Telecommunication and Control*, 2017, Vol. 10, No. 4, Pp. 41–50. DOI: 10.18721/JCSTCS.10404
25. NPN silicon germanium RF transistor NESG3031M14. Available: https://ru.mouser.com/datasheet/2/286/nec_cel_nesg3031m14-1186721.pdf (Accessed: 15.11.2020).
26. AWR design environment getting started guide. Available: https://awrcorp.com/download/faq/english/docs/Getting_Started/Getting_Started.htm (Accessed: 15.11.2020).
27. Keysight technologies CXA X-Series signal analyzer N9000A 9 kHz to 3.0, 7.5, 13.6, or 26.5 GHz. Available: <https://www.keysight.com/ru/ru/assets/7018-02222/data-sheets/5990-4327.pdf> (Accessed: 15.11.2020).
28. HMC732LC4B wideband MMIC VCO with buffer amplifier 6–12 GHz. Available: <https://www.analog.com/media/en/technical-documentation/data-sheets/hmc732.pdf> (Accessed: 15.11.2020).

Received 09.12.2020.

СПИСОК ЛИТЕРАТУРЫ

1. **Grebennikov A.V.** RF and microwave. Transistor oscillator design. John Wiley & Sons, Ltd., 2007. 441 p.
2. **Khanna A.P.S.** State of the art in microwave VCOs // *Microwave Journal*. 2015. Vol. 58. No. 5. Pp. 22–42.
3. **Chenakin A.** Frequency synthesis: Current status and future projections // *Microwave Journal*. 2017. Vol. 60. No. 4. Pp. 22–36.
4. **Chenakin A.** Select a VCO or YIG for a PLL synthesizer // *Microwaves and RF*. 2016. Vol. 55. No. 2. Pp. 2–6.
5. **Garghetti A., Quadrelli F., Bassi M., Mazzanti A.** Impact of the base resistance noise and design of a –190-dBc/Hz FoM Bipolar Class-C VCO // *IEEE Solid-State Circuits Letters*. 2020. Vol. 3. Pp. 90–93. DOI: 10.1109/LSSC.2020.3006484
6. **Горевой А.В.** Выбор генераторов для построения малошумящих СВЧ-синтезаторов // Компоненты и технологии. 2012. № 6. С. 12–17.
7. **Горевой А.В.** Генератор диапазона 1–2 ГГц с повышенной крутизной регулировочной характеристики // Доклады ТУСУРа. 2011. № 1 (23). С. 44–49.
8. **Миловзоров О.В., Панков И.Г.** Электроника. М.: Высшая школа, 2008. 288 с.

9. Datta K., Hashemi H. Waveform engineering in a mm-wave stacked-HBT switching power amplifier // 2017 IEEE Radio Frequency Integrated Circuits Symposium (RFIC). 2017.
10. Stärke P., Steinweg L., Carta C., Ellinger F. Common emitter low noise amplifier with 19 dB Gain for 140 GHz to 220 GHz in 130 nm SiGe // Internat. Conf. on Wireless and Mobile Computing, Networking and Communications (WiMob). 2019.
11. Coen C.T., Ulusoy A.Ç., Song P., Ildefonso A., Kaynak M., Tillack B., Cressler J.D. Design and on-wafer characterization of G-Band SiGe HBT low-noise amplifiers // IEEE Transactions on Microwave Theory and Techniques. 2016. Vol. 64. Iss. 11. Pp. 3631–3642.
12. Pandiev I.M., Stoimenov E.C. Design and development of low-power multistage amplifier laboratory kit for electronic engineering education // 2019 X National Conf. with Internat. Participation (ELECTRONICA). 2019.
13. Pietron D., Butryn I., Wiechowski L., Pleskacz W.A. Design of a wideband low noise amplifier for a FMCW synthetic aperture radar in 130 nm SiGe BiCMOS technology // 25th Internat. Conf. on Mixed Design of Integrated Circuits and System. 2018.
14. Асмолов Г.И., Рожков В.М., Лобов О.П. Усилительные схемы в системах транспортной телематики. М.: МАДИ, 2015. 88 с.
15. Perez J.C., Guardado A.H., Freixedas J.C., Ambrojo J.C.P. A hybrid bipolar wideband VCO with linearized tuning behaviour for a new generation TTC transponder // 48th European Microwave Conference (EuMC). 2018. Pp. 1341–1344.
16. Singha H., Parmara Y.o, Rajb V.B., Pandyac H.M., Kumara J., Mishraa M., Nimala A.T., Sharmaa M.U. Sensitivity enhancement studies of SAW vapor sensor by oscillator tuning using varactor diode // IEEE Sensors Journal. 2016. Vol. 17. No. 5. Pp. 1391–1398.
17. Patel S.S., Gupta S., Ghodgaonkar D. Ku-band novel voltage controlled oscillator microwave integrated circuit with low phase noise // 2014 Internat. Conf. on Computational Intelligence and Communication Networks. 2014. Pp. 74–77.
18. Dyskin A., Wagner S., Kallfass I. A compact resistive quadrature low noise Ka-band VCO SiGe HBT MMIC // 12th German Microwave Conf. 2019.
19. Florian C., D'Angelo S., Scappaviva F. A chip set of low phase noise MMIC VCOs at C, X and Ku-band in InGaP-GaAs HBT technology for satellite telecommunications // 2017 IEEE MTT-S Internat. Microwave Symp. (IMS).
20. Fanori L., Andreani P. Highly efficient class-C CMOS VCOs, including a comparison with class-B VCOs // IEEE Journal of Solid-State Circuits. 2013. Vol. 48. Iss. 7. Pp. 1730–1740.
21. Habbachi N., Boukabache A., Boussetta H., Pons P., Kallala M.A., Besbes K. Analyzes of VCO performances based on RF spiral inductors // 2017 Internat. Conf. on Engineering & MIS (ICEMIS). 2018.
22. Maffezzoni P., Levantino S. Analysis of VCO phase noise in charge-pump phase-locked loops // IEEE Transactions on Circuits and Systems I. 2012. Vol. 59. Iss. 10. Pp. 2165–2175.
23. Никитин А.Б., Хабитуева Е.И. Сверхширокополосный СВЧ-генератор, управляемый напряжением // Радиотехника. 2018. № 1. С. 4–9.
24. Никитин А.Б., Хабитуева Е.И. Особенности разработки сверхширокополосных перестраиваемых генераторов СВЧ диапазона в гибридном исполнении // Научно-технические ведомости СПбГПУ. Информатика. Телекоммуникации. Управление. 2017. Т. 10. № 4. С. 41–50. DOI: 10.18721/JCSTCS.10404
25. NPN silicon germanium RF transistor NESG3031M14 // URL: https://ru.mouser.com/datasheet/2/286/nec_cel_nesg3031m14-1186721.pdf (Дата обращения: 15.11.2020).
26. AWR design environment getting started guide // URL: https://awrcorp.com/download/faq/english/docs/Getting_Started/Getting_Started.htm (Дата обращения: 15.11.2020).
27. Keysight technologies CXA X-Series signal analyzer N9000A 9 kHz to 3.0, 7.5, 13.6, or 26.5 GHz // URL: <https://www.keysight.com/ru/ru/assets/7018-02222/data-sheets/5990-4327.pdf> (Дата обращения: 15.11.2020).

28. HMC732LC4B wideband MMIC VCO with buffer amplifier 6–12 GHz // URL: <https://www.analog.com/media/en/technical-documentation/data-sheets/hmc732.pdf> (Дата обращения: 15.11.2020).

Статья поступила в редакцию 09.12.2020.

THE AUTHORS / СВЕДЕНИЯ ОБ АВТОРАХ

Nikitin Aleksandr B.

Никитин Александр Борисович

E-mail: nikitin@mail.spbstu.ru

Khabitueva Ekaterina I.

Хабитуева Екатерина Исааковна

E-mail: habitueva.ei@edu.spbstu.ru

© Санкт-Петербургский политехнический университет Петра Великого, 2020